

Modeling, Control and Experimental Validation of a Device for Seismic Events Simulation

Paolo Righettini, Roberto Strada, Vittorio Lorenzi, Alberto Oldani, Mattia Rossetti

Abstract—Single and multi-axis shaking tables are an efficient way for the testing of a large number of systems. Among the possible fields of application, the civil engineering field stands out for the testing of structures, or part of them, both on a reduced and on a full scale. This work belongs to this field and concerns the design of a small size (1200 mm x 2000 mm) hydraulic-actuated single-axis shaking table, for the simulation of seismic loads on civil structural elements that weight less than 1200 kg. According to a typical mechatronic approach, the choice of the hydraulic components, the design of the mechanical system and the design of the control system were synergically carried out. Eventually, the system was built and preliminary experimental tests were performed for the evaluation of its functionality.

Keywords—shaking tables, hydraulics, seismics.

I. Introduction

Single and multi-axis shaking tables are an efficient way for the testing of a large number of systems. Their scope ranges in different fields, where civil engineering stands out for the testing of structures, or part of them, both on a reduced and on a full scale [1, 2, 3]. This work belongs to this field and concerns the design of a small size (1200 mm x 2000 mm) hydraulic-operated single-axis shaking table, for the simulation loads due to seismic events on civil structural elements that weight less than 1200 kg. For the definition of the project specifications, reference was made to the seismic actions defined in the UNI EN 1998-1 [4]. In particular, the seismic sample is characterized by an acceleration profile with a peak equal to 0.35 g whose elastic response spectrum shows a 2.8 ratio between S_e and ag , defining a spectrum response similar to the one of type 1, curve C. Besides, the harmonic contents of the seismic sample shows a significant attenuation over 10 Hz (Fig. 1). According to these specifications, a hydraulic-operated system was chosen, in particular, a double rod cylinder (in order to ensure a symmetric behavior of the system) characterized by a 250 mm stroke and by a servo valve with a bandwidth of 100 Hz.

Paolo Righettini, Roberto Strada, Vittorio Lorenzi, Mattia Rossetti
University of Bergamo - Department of Engineering and Applied Sciences, Italy

Alberto Oldani
Mechatronics and Dynamic Devices srl, spin-off company of the University of Bergamo, Italy

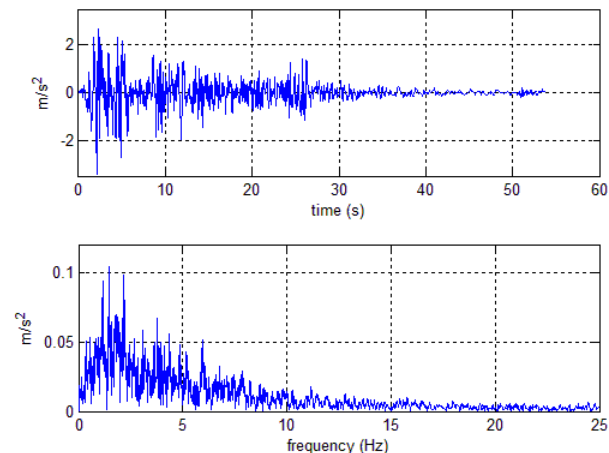


Figure 1. Seismic sample: time history and harmonic content

According to a typical mechatronic approach, the choice of the hydraulic components, the design of the mechanical system and the design of the control system were synergically carried out. Again, from a mechatronic point of view, every components of the system were modeled in order to design a global model of the system able to reproduce, with a good level of accuracy, the actual behavior and being able to evaluate the effectiveness of the control system and the dynamic characteristics of the system itself. Eventually, the system was built and experimentally validated, using both the seismic sample and others acceleration profiles.

II. System Design

The system design involved the choice of the mechanical structure, the selection of the components of the hydraulic-operated system and the design of the control system.

A. Mechanical Structure

As previously mentioned, the design specifications require the development of a small size system; Fig. 2 shows the 3D model of the system where are pointed out the elements composing the system. In particular: (A) moving platform for specimens housing (1200 mm x 2000 mm); (B) rail guides for the coupling with the fixed base (C) using linear ball type guideways (D); hydraulic actuator for the movement of the mobile base attached to it using the connection (F); (G) hydraulic system for the actuator supply; (H) mechanical end-stroke; (I) displacement potentiometric transducer.

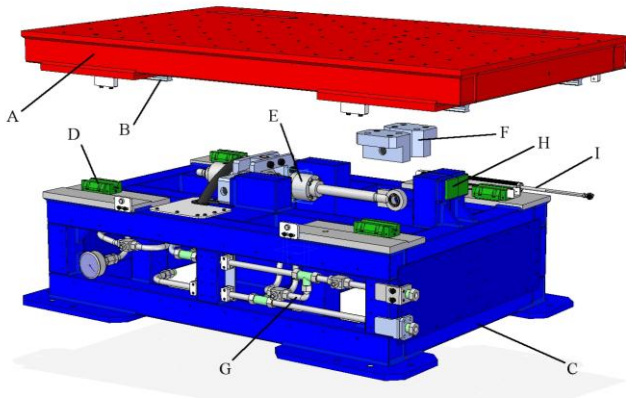


Figure 2. 3D model

The fixed base (C) is built of square pipes welded each other dealing to a high stiffness structure. For the frame design, FEM analysis was done at the most heaviest conditions, i.e. when the mobile platform bumps against the mechanical end-stroke with the hydraulic actuator exerting the maximum possible force, which is 19000 N.

Fig. 3 and Fig. 4 show some results obtained from the FEM software MSC Nastran, combined to MSC Patran as a pre- and post-processor. In particular, the analysis was focused on the most stressed part of the system, i.e. on the mechanical end-stroke; in Fig. 3 are shown the results obtained from the actuator push phase, while in Fig. 4 are shown the results

relative to the pulling phase. As can be seen from the figures, the structure is fully verified.

The mobile base was analyzed using a FEA method too, with the purpose of evaluating the effect of a specimen when, fixed to the base, exerts the maximum moment defined in the design specifications. In particular, it was considered the maximum value of the specimen mass (1200 kg) with the center of mass positioned at 1 m of height from the mobile base and subjected to an acceleration of 0.35 g; the resulting action was increased for safety reasons.

In Fig. 5 and Fig. 6 are shown the results of these analysis both in terms of stress (fig. 5) and of strain (fig. 6). In this case as well, the structure results fully verified.

Being the application typically dynamic, also modal analysis was carried out, using the same FEM code, both for the fixed base and for the mobile one. The results are shown in Fig.7 and Fig. 8 where is pointed out that for the fixed base (fig. 7) the first mode with components in the direction of the motion is the III, characterized by a frequency of 296 Hz, which is very far from the maximum working frequency of the system (10 Hz).

B. Drive system

As previously discussed and shown in Fig. 2, the system is actuated by a hydraulic actuator driven by a servo valve. The actuator is a *Bosch-Rexroth* double-rod cylinder CGH2 series with a 250 mm stroke, 50 mm bore diameter and a 36 mm rod

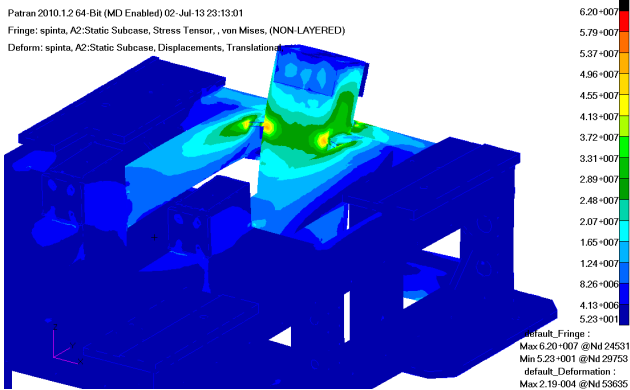


Figure 3. Frame FEM analysis: push phase

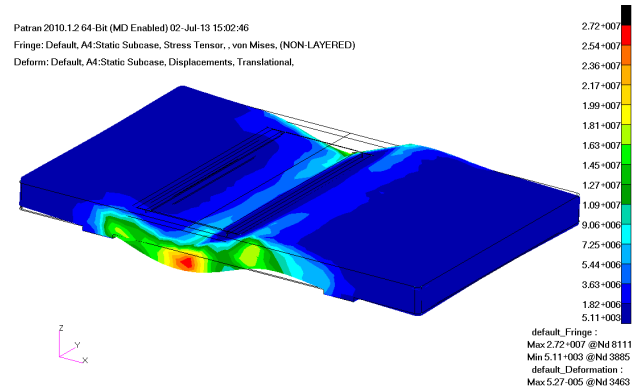


Figure 5. Mobile base FEM analysis: stress

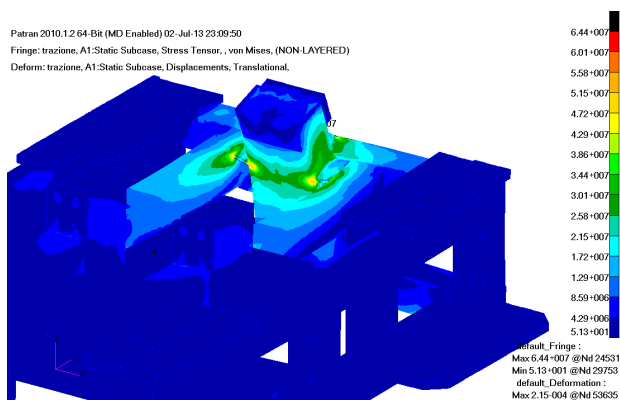


Figure 4. Frame FEM analysis: pull phase

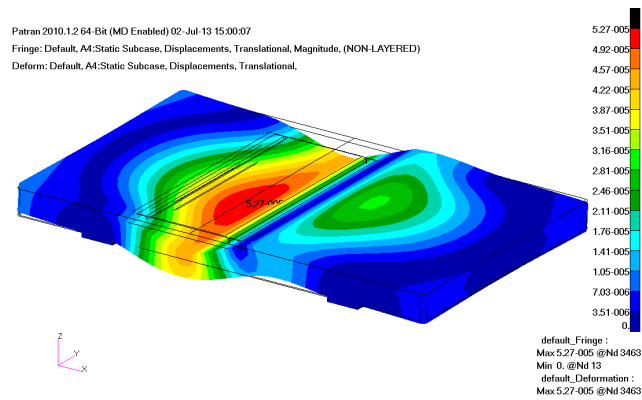


Figure 6. Mobile base FEM analysis: strain

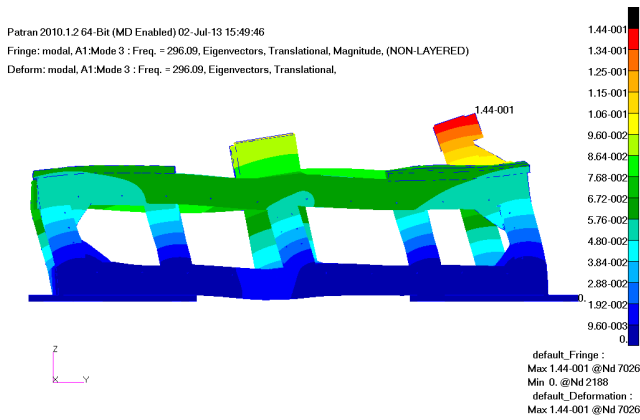


Figure 7. Fixed base modal analysis: III mode, 296 Hz

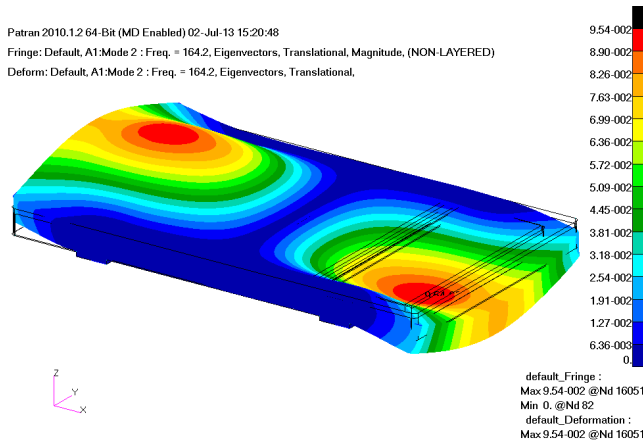


Figure 8. Mobile base modal analysis: II mode, 164 Hz

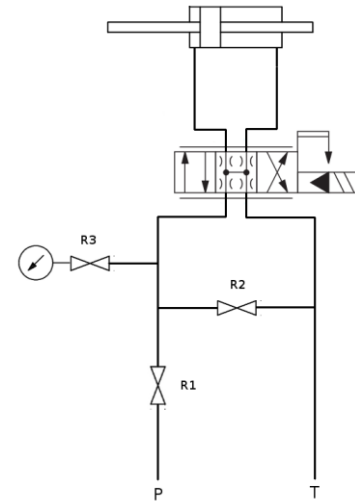


Figure 9. Hydraulic scheme

Δ indicates the variation with respect to the chosen working condition;

R defines the working condition.

In terms of Laplace transforms, the previous equation becomes:

$$Q_L = K_q X_v - K_c P_L \quad (2)$$

Neglecting, at this stage, the leakages in the cylinder and friction forces, the following equations apply for the actuator chambers and the piston, still expressed in terms of Laplace transforms:

$$Q_L = A X_s + \frac{V_t}{4\epsilon_a} P_L s, \quad P_L A = M X s^2 \quad (3)$$

where:

A is the piston area;

X is the piston displacement;

V_t is the actuator total volume;

ϵ_a is the fluid bulk modulus.

From (2) and (3) is obtained the transfer function between the valve opening and the piston displacement:

$$\frac{X}{X_v} = \frac{\frac{K_q}{A}}{s \left(\frac{s^2}{\omega_h^2} + \frac{2\zeta_h}{\omega_h} s + 1 \right)} \quad (4)$$

where:

$$\omega_h = \sqrt{\frac{4\epsilon_a A^2}{V_t M}} \quad (5)$$

is the natural frequency and

diameter. The servo valve (*Bosch-Rexroth* 4WS.2E series) has an open centers configuration and is characterized by a 20 l/min nominal flow and by a bandwidth of about 100 Hz.

Fig. 9 shows the hydraulic scheme of the plant installed on the device; in addition to the servo valve and to the cylinder, there are a ball valve (R1) for the supply shut off, a ball valve (R2) for by-passing the actuator and a ball valve (R3) for the plant supply pressure display.

For the drive system choice, the dynamic performances were evaluated using the well-known linear model [5]. Based on this model, the servo valve behavior, near a working condition, can be described by the following equation:

$$\Delta q_L = K_q \Delta x_v - K_c \Delta p_L \quad (1)$$

where:

q_L is the line flow rate;

x_v is the valve opening;

p_L is the pressure drop on the actuator;

$K_q = (\partial q_L / \partial x_v)_R$ is the flow coefficient (gain);

$K_c = -(\partial q_L / \partial p_L)_R$ is the flow-pressure coefficient;

$$\zeta_h = \frac{K_c}{A} \sqrt{\frac{\epsilon_s M}{V_t}} \quad (6)$$

is the damping factor of the servo valve/actuator system.

The parameters needed for the definition of the transfer function were obtained from the datasheet of the respective components. Generally, K_q and K_c coefficients are not included in the servo valve datasheets, so they can be calculated from the servo valve characteristic curves, shown in Fig. 10 and Fig. 11, drawn from datasheet.

The Bode diagram shown in Fig. 12 was determined using the parameters obtained from the datasheets in the expression of the transfer function. In this diagram it can be noticed that the system is configured in such a way that its dynamic performances allow to ensure the maximum desired working frequency (10 Hz).

C. Control system

As previously mentioned, the hydraulic actuator needs a control system in order to allow the base follow the desired

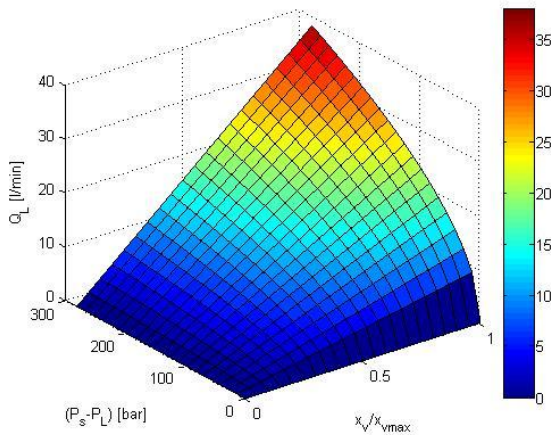


Figure 11. Servo valve characteristic surface

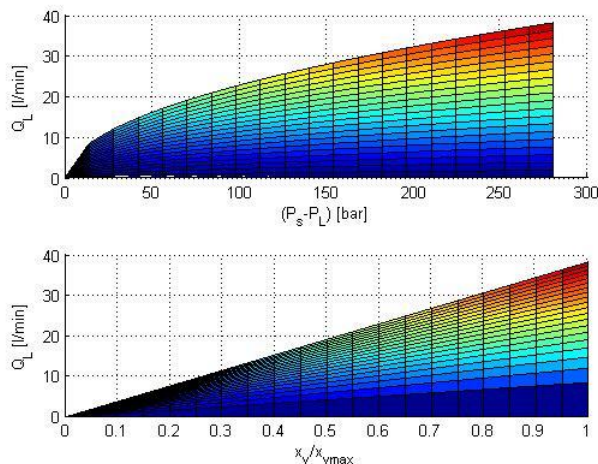


Figure 10. Servo valve characteristics curves

acceleration profile; hence the system needs to be controlled with an appropriate closed-loop algorithm. As said before, the displacement of the mobile base is measured by means of a linear potentiometer.

The control system design is still based on the linear model of the system; in particular, considering the transfer function (4), a closed-loop displacement control system is implemented. As shown in Fig.13, the feedback of the system is the signal coming from the potentiometer.

Besides, as shown in Fig.13, the controller chosen is a PD (proportional-derivative) one. The controller parameters choice is based on the position of the complex conjugate poles of the transfer function in the closed-loop configuration. The parameters were chosen in order that the frequency and the damping obtained could ensure that the project specifications were respected and that noise on the signals could be filtered.

The transfer function in the closed-loop configuration is:

$$\frac{X}{X_0} = \frac{\frac{K_q}{A} (K_p + K_D s)}{s^3 + \frac{2\zeta_h}{\omega_h} s^2 + \left(\frac{K_q}{A} K_D + 1\right) s + \frac{K_q K_p}{A}} \quad (7)$$

III. Modeling and Simulation

Before starting with the operational phase, simulations of the system in Matlab/Simulink environment were done in order to validate the design choices. The simulations were done in the time domain on more accurate models than the linear ones used for the components choice. In particular, these models

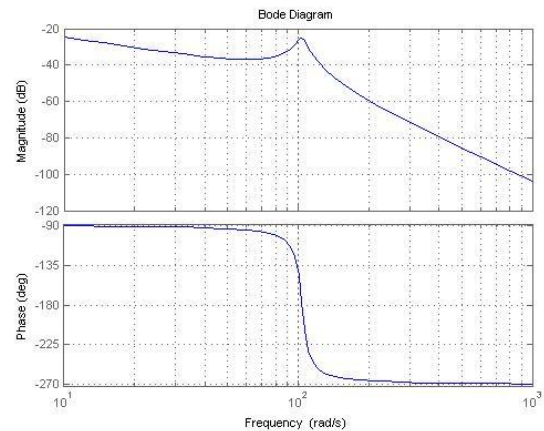


Figure 12. Transfer function X/X_0



Figure 13. System control scheme

take into account the non-linear characteristics of the servo valve, its open centers configuration and the cylinder leakages.

For the servo valve:

$$q_L = C_d \omega (\text{sign}(x_v) U + x_v) \sqrt{\frac{1}{\rho} (p_s - \text{sign}(x_v) p_L)} - C_d \omega (-\text{sign}(x_v) U - x_v) \sqrt{\frac{1}{\rho} (p_s + \text{sign}(x_v) p_L)} \quad (8)$$

Where:

$U = 0.5\% x_{v \max}$ is the spool underlap region (from datasheet)

C_d is the discharge coefficient;

ω is the area gradient;

x_v is the valve opening;

ρ is the fluid density;

p_s is the supply pressure;

It can be noticed that the discharge coefficient C_d and the area gradient ω , can be treated like a single parameter that connects the flow to the pressure drop that can be obtained from the graphics in Fig.11.

Defining the continuity flow equations for both chambers, the line flow q_L can be expressed as:

$$q_L = A \dot{x} + \left(C_{im} + \frac{C_{em}}{2} \right) p_L + \frac{V_t}{4 \epsilon_a} \frac{dp_L}{dt} \quad (9)$$

On the piston there are no external actions and, considering the use of linear ball type guideways, the frictions forces can be neglected too; the dynamic equilibrium equation of the forces acting on the piston results in the following expression:

$$p_L A = M \ddot{x} \quad (10)$$

where M is the total mass (mobile base plus the specimen) moved by the actuator. Equations (8), (9) and (10) represent the non-linear model of the servo valve/actuator system. For the evaluation of the leakages reference was made at the data found in literature [5].

For example, Fig.14 and Fig. 15 show the results obtained from a simulation that concerns the time history of the acceleration of a real seismic event.

As it can be noticed in the graphics represented in figure 14, the comparison between the desired acceleration and the one obtained from the simulation is a good approximation, with a maximum error of about 0.3 m/s^2 which is about the 10% of the maximum value of acceleration, moreover it is limited only to a few instants.

Fig. 15 shows that the values of the valve opening and of the pressure drop are acceptable as well, staying below the allowed values. In particular, the opening never exceeds the maximum value and the pressure jump never exceeds 210 bar ,

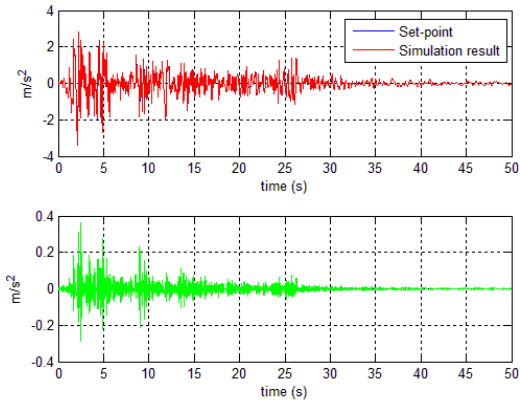


Figure 14. Acceleration (sample seismic event)

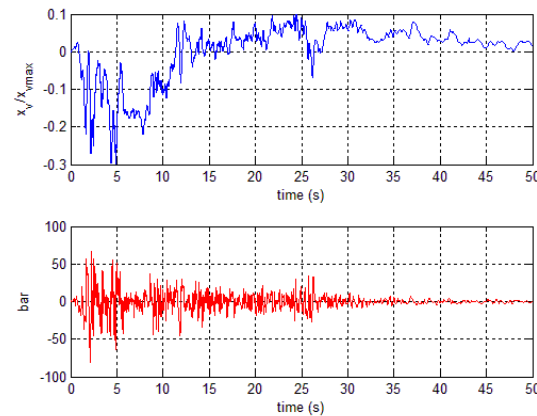


Figure 15. Valve opening ratio ($X_v/X_{v \max}$), pressure drop.

which is the maximum pressure of the plant that will supply the device.

IV. Experimental tests

After designing, modeling and simulation stages, the shaking table was built; Fig. 16 shows the device.

Preliminary tests shown that the mechanical configuration of the system satisfies the design specifications: in particular, thanks to the optimal alignment of the linear ball type guideways, friction forces are negligible compared to inertial loads.

Tests for the experimental evaluation of the dynamic performances are currently being done using both acceleration profiles from real seismic events and other profiles for the evaluation of the maximum performances obtainable. As an example, Fig. 17 and Fig. 18 show the results of some preliminary tests. In particular, Fig. 17 shows the actual acceleration of the mobile base for an acceleration set point, sum of 1 Hz and 8 Hz harmonics. The spectrum analysis of the signal shows that the measured acceleration is characterized by the expected frequencies. Fig. 18 concerns the device response to a single frequency set point and shows that the



Figure 16. Physical system

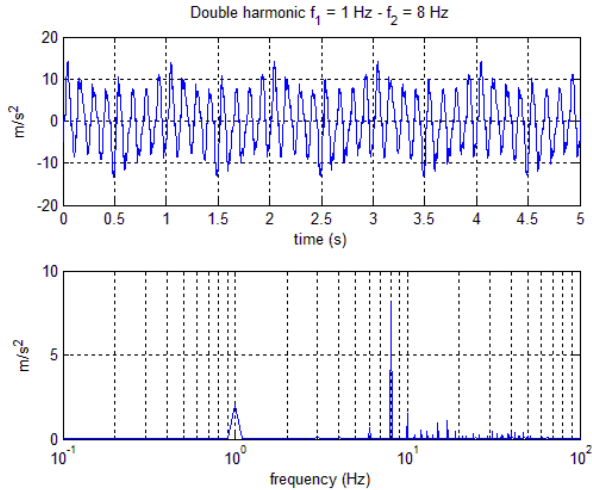


Figure 17. Measured acceleration time history and spectrum analysis for a double harmonic set point.

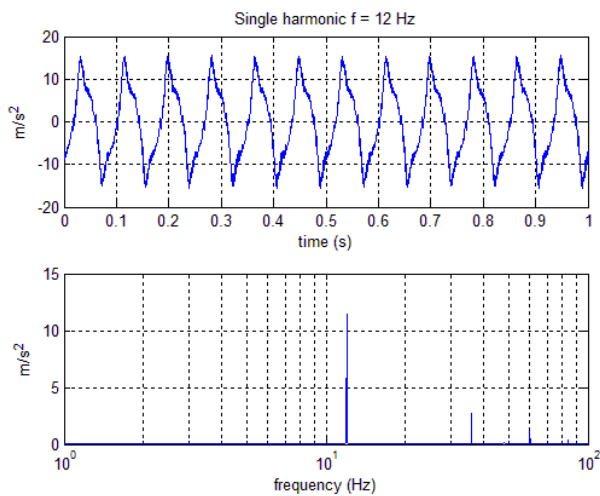


Figure 18. Measured acceleration time history and spectrum analysis for a single harmonic set point.

system is capable to accurately reproduce the input signals, even at a frequency (12 Hz) higher than the design one (10 Hz).

v. Conclusions

This paper concerns the designing of a 1 degree of freedom hydraulic-operated shaking table for seismic events simulation

of components and specimen in the civil field. The project was developed using a typical mechatronic approach that results in high performances, thanks to the interaction between the components of the system. In this context, the designing has concerned the mechanical aspects, the hydraulic drive system and the control system. For the selection and validation of the components, was set up a model of the system as a whole and were made simulations that shows the honesty of the made choices. The system was realized and it is now under testing for the experimental validation, both in terms of functionalities and of evaluation of the obtainable dynamic performances. Some preliminary tests carried out with harmonic signals show that the system is capable to accurately reproduce the acceleration set point, characterized by frequencies even higher than the design one.

References

- [1] Thulin Jr., F.A., “Shaker for seismic testing”, in Proceedings of the 1985 Pressure Vessels and Piping Conference. Piping, Feedwater Heater Operation, and Pumps. (71-76, New Orleans, 1985), LA, USA.
- [2] Eunjong Yu, Daniel H. Whang, Joel P. Conte, Jonathan P. Stewart and John W. Wallace, “Forced vibration testing of buildings using linear shaker seismic simulation (LSSS) testing method”, *Earthquake Engineering and Structural Dynamics* 2005; 34:737-761.
- [3] D.P. Newell, H. Dai, M.K. Sain, P. Quast, B.F. Spencer Jr., “Nonlinear Modeling and Control of a Hydraulic Seismic Simulator”, *Proceedings American Control Conference*, Pages 801-805, June 1995.
- [4] UNI, UNI EN 1998-1, “Eurocodice 8 – Progettazione delle strutture per la resistenza sismica – Parte 1: Regole generali, azioni sismiche e regole per gli edifici” (2005).
- [5] Merritt H., “Hydraulic control systems”, John Wiley & Sons, (1967).

About Authors:



Paolo Righettini is Associate Professor of Applied Mechanics. Research interests: Design of complex mechatronic systems, dynamics and vibration control of mechanical systems



Roberto Strada is Assistant Professor of Applied Mechanics. Research interests: mechatronics, electro-hydraulic driving systems, dynamics of mechanical systems



Vittorio Lorenzi is Associate Professor of Applied Mechanics. Research interests: Multybody systems dynamics, Vehicle dynamics.



Alberto Oldani is a PhD Engineer. Field of interests: Multybody systems dynamics, Control of mechatronic systems.



Mattia Rossetti is a PhD student. Field of interests: Control of mechatronic systems, Vision systems.